J. Fluid Mech. (2007), *vol.* 583, *pp.* 459–464.
doi:10.1017/S0022112007006726 Printed in the United Kingdom

A note on the similarity between the normal-field instability in ferrofluids and the thermocapillary instability

SANG W. JOO

School of Mechanical Engineering, Yeungnam University, Gyongsan 712-749, Korea

(Received 26 February 2007 and in revised form 30 April 2007)

A striking resemblance between the normal-field instability in ferromagnetic fluids and the interfacial mode of the thermocapillary instability in viscous fluids is presented. A nonlinear evolution equation describing the dynamics of the free surface for a ferrofluid layer subject to a uniform normal magnetic field is derived, and compared to that for a thin viscous layer heated from below. Their similarity predicts the possibility of mutual nonlinear stability control.

1. Thermocapillary instability

There are two distinct modes of thermocapillary instability in liquid layers heated from below. Through a careful linear stability analysis, Goussis & Kelly (1990) report that thin layers are subject to the interfacial mode which is accompanied by surface corrugations, while thick layers become unstable by the convective mode which does not require surface deformations. The dynamics of a thin liquid layer thus can be approximated by a nonlinear evolution equation of the Benney (1966) type, which is derived by applying the long-wave asymptotics. For a layer of mean thickness d, kinematic viscosity ν, density ρ, thermal conductivity k, and surface-tension coefficient γ (with the air), the evolution equation is written as

$$h_t + \frac{BiM}{P}\left[\frac{h^2 h_x}{(1+Bih)^2}\right]_x + S(h^3 h_{xxx})_x = 0, \tag{1.1}$$

where $h(x,t)$ is the local layer thickness non-dimensionalized by d and subscripts denote partial differentiations. Here a viscous time scale d^2/ν is used. The non-dimensional parameters are the Biot number $Bi = hd/k$, Marangoni number $M = d\beta\Delta T/(2\rho\nu k)$, Prandtl number P, and surface-tension number $S = \gamma d/(3\rho\nu^2)$, where h, β, and ΔT are the heat-transfer coefficient, thermocapillary coefficient, and temperature difference imposed, respectively.

Numerical integration of the evolution equation (1.1) with appropriate boundary conditions is a convenient way of studying the nonlinear flow development for layers subject to thermocapillary instability. By comparing with a finite-element computation Krishnamoorthy, Ramaswamy & Joo (1995) report that (1.1) is an excellent approximation of the original free-boundary problem unless the free surface locally steepens significantly, in which case (1.1) overestimates surface slopes and peaks. Substantially more nonlinearities need to be included then. A weakly nonlinear analysis can be performed by writing the solution to (1.1) in a Fourier series and extracting a dynamical system for the Fourier coefficients. Various tools then become available for predicting the fate of the heated layer.

2. Normal-field instability

A uniform magnetic field applied perpendicular to a ferrofluid layer can cause spontaneous corrugations of the surface, which is reported by Cowley & Rosensweig (1967) as the normal-field instability. In addition to hydrodynamic equations the system is described by Ampere's law $\nabla \times \boldsymbol{H} = 0$ for the magnetic field $\boldsymbol{H}$ and the Maxwell equation $\nabla \cdot \boldsymbol{B} = 0$ for the magnetic induction $\boldsymbol{B}$ in all phases. The magnetic induction is related to the magnetic field by $\boldsymbol{B} = \mu \boldsymbol{H}$, where μ is the magnetic permeability with a minimum value μ_0 for vacuum. The magnetic susceptibility of a medium then can be defined as $\mu/\mu_0 - 1 \equiv \alpha - 1$, which vanishes for a non-magnetic material. The normal-field instability necessarily accompanies free-surface deformations, and occurs with long waves. A finite-element computation performed by Matthies & Tobiska (2005) for the fully coupled system confirmed the linear analysis and showed some nonlinear flow developments.

As a way of avoiding enormous computational effort with the full system and further studying the normal-field instability, we can apply the same long-wave asymptotics as those used for deriving (1.1). All three phases (substrate, ferrofluid, and air) must be considered, and the resulting analysis is somewhat more involved. It is nevertheless quite straightforward. If we use the constitutive relationship

$$\boldsymbol{\sigma} = -\left(p + \frac{\mu_0}{2} |\boldsymbol{H}|^2 \right) + \rho\nu(\nabla \boldsymbol{u} + \nabla \boldsymbol{u}^T) + \boldsymbol{B}\boldsymbol{H}, \tag{2.1}$$

where $\boldsymbol{\sigma}$ and $\boldsymbol{u}$ are stress tensor and velocity vector, respectively, and assume that the magnetic susceptibility of the air and the substrate are zero, the evolution equation becomes, as shown in the Appendix,

$$h_t + \frac{1}{2} H_0^2 \left(1 - \frac{1}{\alpha} \right) (h^2 h_x)_x + S(h^3 h_{xxx})_x = 0, \tag{2.2}$$

where the intensity of the uniform magnetic field imposed $\bar{H}_0$ is non-dimensionalized as $H_0^2 = \mu d^2 \bar{H}_0^2/(\rho\nu^2)$. For a ferrofluid $\alpha > 1$, and so the coefficient $A \equiv H_0^2(1 - 1/\alpha)/2$ for the diffusive term is positive, giving rise to the normal-field instability.

It is interesting to note that for common small-Biot-number flows, where $Bih \ll 1$, (1.1) and (2.2) are almost identical. The onset of instability and subsequent flow developments can be identically understood using BiM/P since $(1 + Bih) \approx 1$. Dynamical system approaches for the thermocapillary instability would apply to the normal-field instability as well. Numerical integrations of (2.2) have indeed shown that all the important features in (1.1), such as period-doubling bifurcations and incipient rupture, are captured in (2.2). We will not repeat these results here. The evolution toward typical spiked surfaces under normal magnetic fields is simulated instead. Among numerous cases investigated, the ones obtained by stretching (2.2) to its limit are presented.

Figure 1 shows how an initially smooth drop would evolve after a magnetic field is switched on. For clarity, only half of the drop is shown, with its edge and the contact angle fixed in their initial states. The smooth line showing $h = 1$ at the centre ($x = 0$) is the initial shape, while the line showing multiple incipient ruptures and the largest secondary peaks is for the instant at which the numerical integration of (2.2) is terminated due to rupture ($h < 10^{-6}$). A fourth-order central-difference scheme is used in space with second-order fully implicit time marching and an absolute error bound of 10^{-6}. The formation of the spikes and appearance of the secondary spikes between the main spikes can be understood by analogy to the corresponding thermocapillary

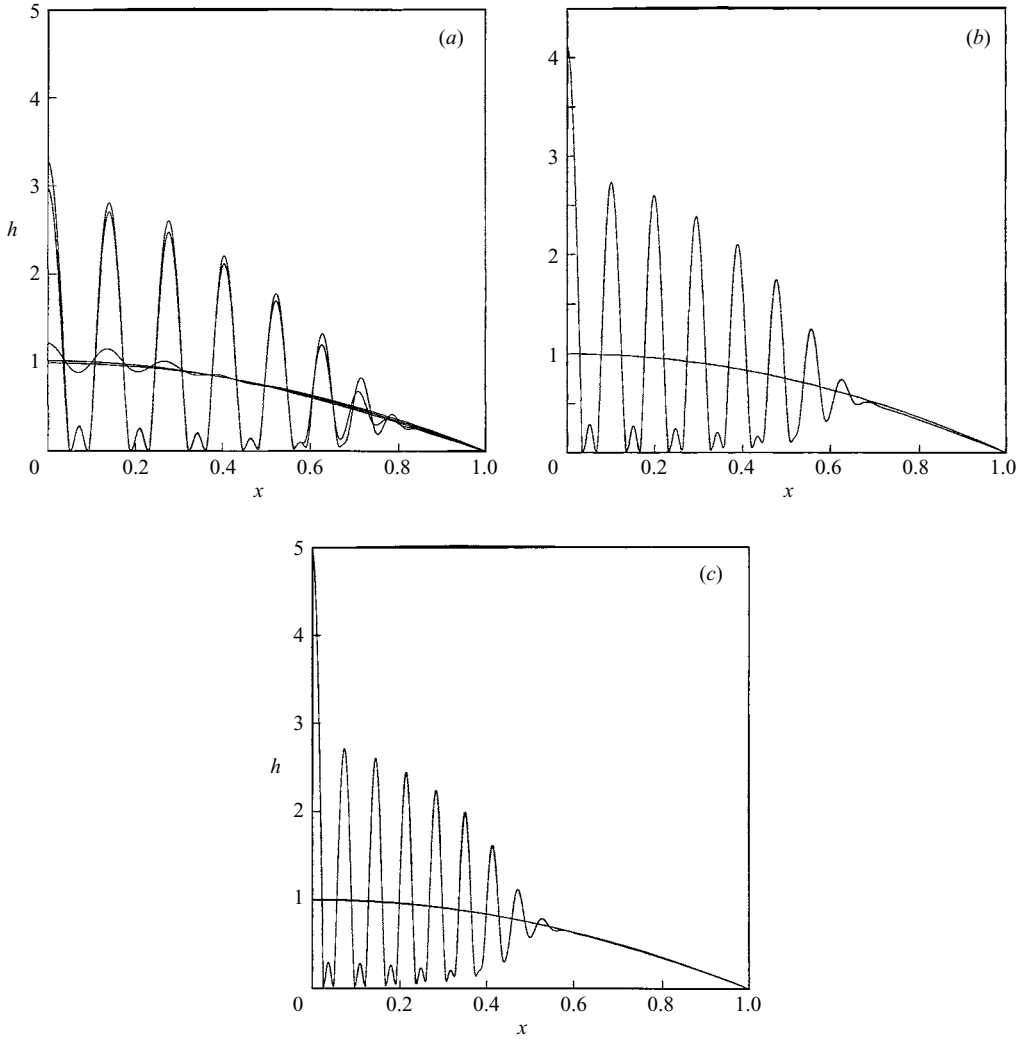

FIGURE 1. Shape of a ferrofluid drop at $t = 0$ and near rupture time (*a*) $t = 570$; (*b*) $t = 130$; (*c*) $t = 32$. $A = S = 1$.

instability, which is discussed by Joo, Davis & Bankoff (1993) for flows with periodic disturbances. In figure 1(*a*) surface shapes at an early and a late stage of the evolution are shown additionally. With the increase of the magnetic field, the rate of growth of the spikes and of the incipient rupture increases rapidly. The rupture time then decreases rapidly with A, and so the vertical dimension of the spikes at the final time step shown indicates little dependence on the magnetic field. The horizontal dimension of the spikes appears to decrease with the magnetic field. The number of conspicuous spikes, however, is not proportional to A. The decrease in the horizontal dimension is achieved rather by concentrated spike population near the centre of the drop.

In figure 2 an evolution of a continuous ferrofluid film is shown. The flat line with a small dimple at the centre shows one period of the initial surface shape, while the highly corrugated line represents that near rupture. The amplitude of the spikes developed is maximum near the centre, and decreases with the distance from the initial

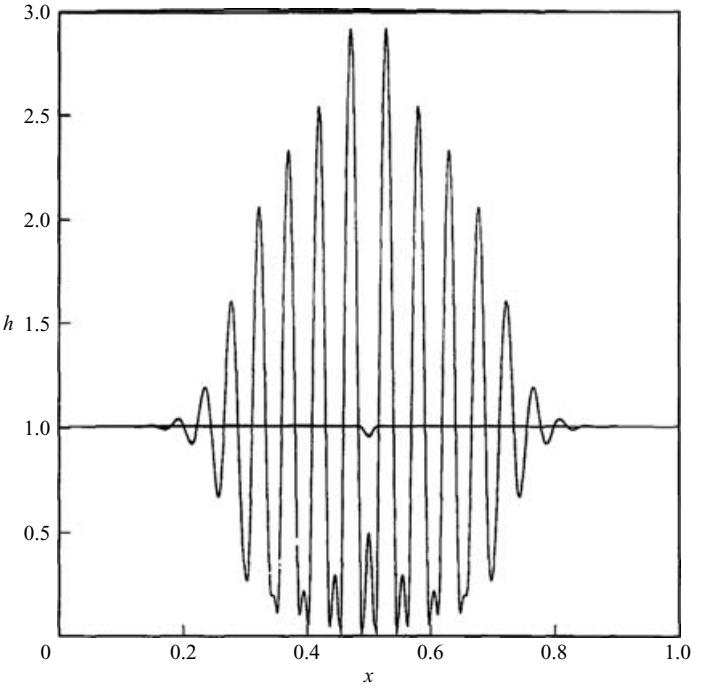

FIGURE 2. Shape of a horizontally periodic ferrofluid layer at $t = 0$ and rupture time $t = 83.6$ for $A = S = 1$.

disturbance. The number of spikes and their horizontal dimension, however, appear to be independent of the location and amplitude of the small initial disturbance. Secondary spikes are seen near the centre. Their amplitude again decreases with the distance from the initial disturbance. Investigations of the flow development beyond rupture require modification of (2.2), as discussed in the Appendix.

3. Concluding remarks

The fixed-contact-line condition in figure 1 can be relaxed by modifying (2.2) to include the dynamics of moving contact lines. Break-up of ferrofluid drops under a normal field, or the topological instability, can then be simulated. This generalization, however, is beyond the scope the present note, and will be reported elsewhere.

In a horizontal layer, the hydrostatic pressure would stabilize the interfacial instability, and thus require critical values of A or BiM/P for the onset of the instability. In both (1.1) and (2.2) this hydrostatic stabilization can be realized by adding a term $-G(h^3 h_x)_x/3$ to the left-hand side, where $G = gd^3/\nu$ is a measure of the layer thickness. In the evolution equations of the type discussed here nonlinear ingredients are introduced through linear superpositions. Additional effects, such as inclination, evaporation, or molecular forces, thus can be modelled without altering the existing terms. If one wishes to include thermocapillary in (2.2), simply adding the second term of (1.1) will suffice. The resulting evolution equation indicates, among other features, that the normal-field instability can be suppressed completely by sufficiently heating the layer from above ($M < 0$). In addition to this mutual stability control, the similarity of (1.1) and (2.2) suggests the possibility of simulating a thermocapillary flow in thin layers with a ferrofluid experiment.

Equation (2.2) can easily be extended to three dimensions, as done by Joo *et al.* (1993) for a generalized version of (1.1), and then be used to study pattern formations under a normal field. Combined with the contact-line dynamics mentioned above, this may become a useful tool for further investigating the topological instability and the labyrinthine instability, discussed among others by Rosensweig, Zahn & Schumovich (1983).

This work is supported by the National Center for Nanomaterials Technology of Pohang through Yeungnam University.

Appendix. Derivation of the evolution equation (2.2)

The full system is described by the magnetostatic equations (Ampere's law and the Maxwell equation) in all three phases (air, ferrofluid layer, and solid substrate) and the hydrodynamic equations

$$\nabla \cdot \boldsymbol{u} = 0 \quad \text{and} \quad \rho \frac{\mathrm{D}\boldsymbol{u}}{\mathrm{D}t} = \nabla \cdot \boldsymbol{\sigma} \tag{A 1}$$

in the ferrofluid layer. Associated boundary conditions are $[[\boldsymbol{n} \times \boldsymbol{H}]] = 0$ and $[[\boldsymbol{n} \cdot \boldsymbol{B}]] = 0$ at both interfaces, where the double brackets denote a jump in quantities and $\boldsymbol{n}$ is the unit normal vector of the interface. At the liquid/solid interface $\boldsymbol{u} = 0$, and the normal and tangential component of surface traction balance $[[\boldsymbol{n} \cdot \boldsymbol{\sigma} \cdot \boldsymbol{n}]] = \gamma \nabla \cdot \boldsymbol{n}$ and $[[\boldsymbol{t} \cdot \boldsymbol{\sigma} \cdot \boldsymbol{n}]] = 0$ are imposed at the air/liquid interface $y = h$, the location of which is determined by the kinematic condition

$$h_t + \frac{\partial}{\partial x} \int_0^h u \, \mathrm{d}y = 0, \tag{A 2}$$

where u is the x-component of the velocity vector.

We non-dimensionalize the above system using d, d^2/ν, ν/d, and $\rho\nu^2/d^2$ as length, time, velocity, and stress scale, respectively, and apply a lubrication-type approximation by rescaling the resulting system with $\xi = \epsilon x$ and $\tau = \epsilon t$, where ϵ is the smallness parameter, defined as the ratio of a typical horizontal length scale to d. We then expand all dependent variables, except h, for small ϵ: $u(\xi, y, \tau) = u_0(\xi, y, \tau) + \epsilon u_1(\xi, y, \tau) + \cdots$ for example, where identical expressions are used for non-dimensional quantities for convenience. If we substitute these expansions into the rescaled system, solutions to all dependent variables can be obtained sequentially by solving linearized equations at each order. After substituting the second-order solution $u = u_0 + \epsilon u_1$ into the rescaled version of (A 2) we obtain the evolution equation (2.2) by changing ξ and τ to the original non-dimensional x and t. As in (1.1), the surface tension parameter S is retained by setting it to be of order ϵ^{-2}.

If one wishes to study the topological instability, (2.2) must be modified to allow contact-line motions. The boundary condition $\boldsymbol{u} = 0$ at the liquid/solid interface then is modified with a slip model to yield $\boldsymbol{u} = (\beta u_y / h^n, 0)$, where β is the slip coefficient and n (> 1) is an appropriate integer. The amended evolution equation becomes

$$h_t + A[(h^2 + 2\beta h^{1-n})h_x]_x + S[(h^3 + 3\beta h^{2-n})h_{xxx}]_x = 0. \tag{A 3}$$

REFERENCES

Benney, D. J. 1966 Long waves on liquid films. *J. Math. Phys.* **45**, 150–155.

Cowley, M. D. & Rosensweig, R. E. 1967 The interfacial stability of a ferromagnetic fluid. *J. Fluid Mech.* **30**, 671–688.

Goussis, D. A. & Kelly, R. E. 1990 On the thermocapillary instabilities in a liquid layer heated from below. *Intl J. Heat Mass Transfer* **33**, 2237–2245.

Joo, S. W., Davis, S. H. & Bankoff, S. G. 1993 Two- and three-dimensional instabilities and rupture of thin liquid films falling on heated inclined plate. *Nuclear Engng Design* **141**, 225-236.

Krishnamoorthy, S., Ramswamy, B. & Joo, S. W. 1995 Nonlinear wave formation and rupture in heated falling films: A full-scale direct numerical simulation. *Phys. Fluids* **7**, 2291–2294.

Matthies, G. & Tobiska, L. 2005 Numerical simulation of normal-field instability in the static and dynamic case. *J. Magn. Magn. Mater*. **289**, 346–349.

Rosensweig, R. E., Zahn, M. & Schumovich, M. 1983 Labyrinthine instability in magnetic and dielectric fluids. *J. Magn. Magn. Mater*. **39**, 127–132.